

Controlled synthesis of anisotropic gold nanoparticles by a simple polyol process and their related optical properties.

Kais Gharbi^{1,2}, Amine Mezni¹, Vincent Collière², Karine Philippot², Catherine Amiens², Diana Ciuculescu-Pradines², and Leila Samia Smiri^{1*}.

¹ *Unité de recherche UR11ES30, Faculté des Sciences de Bizerte, Université de Carthage, 7021, Bizerte, Tunisia.*

² *CNRS, LCC (Laboratoire de Chimie de Coordination), 205 route de Narbonne, BP 44099, 31077 TOULOUSE Cedex 4, France ; Université de Toulouse, UPS, INPT, F-31077 Toulouse Cedex 4, France*

(Received: 04 September 2017, accepted: 01 November 2017)

Abstract: The understanding of factors influencing the nucleation and growth of gold nanoparticles for morphological and size control requires a simple and handy synthesis protocol. Gold nanoparticles were prepared by a polyol process using Triethylene glycol (TrEG) or 1,3-propanediol (1.3-POD) as a solvent. A whole comparative study emphasized the solvent effect on the nanoparticle shape control. In addition, beside the well known potential of the polyol process to provide biocompatible nanoparticles with a large choice of anisotropic shape, we were able here to decrease their size. Hexagonal and triangular plates of ca. 50 nm and nanocubes of ca. 30 nm were formed, allowing the access of a range of sizes scarcely obtained in a polyol process. These gold nanoparticles might have a large panel of biomedical applications given their plasmonic properties, biocompatibility and stability.

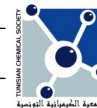
Keywords: Gold nanoparticles, morphological and size control, polyol process, solvent effect.

INTRODUCTION

Gold nanoparticles (AuNPs) are attractive materials due to their unique chemical and physical properties that make them suitable for a very wide range of applications[1-4] such as catalysis[5], optical devices[6], bioengineering, theranostics [7,8], photothermal therapy[9], etc. Au NPs are able to quickly convert absorbed optical energy into thermal energy in limited time span, making them excellent hyperthermia mediators for the cancer treatment[10-13]. The use of Au NPs in hyperthermia application is mainly conditioned by a strong Surface Plasmon Resonance (SPR) localized at near infrared region[14]. Moreover, it is well known that the plasmon resonance wavelength of gold nanoparticles strongly depends on their sizes and shapes (rod[15], cube[16], triangle[17], prism[18], star[19]...). But, despite the technological importance of these nanocrystals and the extended efforts to study them, attempts to synthetically and systematically control their shapes and properties have met limited success. The reduction of metal salts is the most well-

known and frequently used method to synthesize AuNPs. Gold nanorods, synthesized by El-Sayed *and al.*, are the ideal example of anisotropic nanoparticles which absorb in NIR wavelength region[20]. Unfortunately, the cetyltrimethylammonium bromide (CTAB) used in this synthesis is strongly not advised and should be excluded for biomedical applications because of its acute toxicity[21]. Instead, polyvinylpyrrolidone (PVP) is a biocompatible stabilizer most commonly used in the synthesis of metal nanocrystals[22-24]. Numerous studies highlighted the role of PVP as capping agent, shape-directing reagent and even as reducing agent[25]. Polyols(diethylene glycol (DEG), triethylene glycol (TrEG), tetraethylene glycol (TEG), polyethylene glycol (PEG), etc.), are interesting solvents for the synthesis of nanoparticles due to their high dielectric constants, viscosities, boiling points and their strong ability to dissolve metal salts and polar stabilizers in high concentrations[26,27]. Gold nanocrystals with different shapes and sizes have already been produced in polyol medium and in the presence of

* Corresponding author, e-mail address : lsmiri@gmail.com



PVP[28-31]. In a previous work we have studied the optical properties of triangular gold nanoprisms with an average edge length of 150 nm, synthesized in triethylene glycol (TrEG) with PVP as capping agent [31].

Now, we report on a series of comparative experiments based on our previous polyol process. Different conditions were tested, either with triethylene glycol (TrEG) or 1,3-propanediol (1.3-POD) as a medium, PVP as the stabilizing agent, different PVP/gold salt ratios and a mild temperature of reaction. The aim of this work was to study the role of different synthesis parameters on the anisotropic growth orientation of gold nanoparticles. The resulting nanoparticles, synthesized by using biocompatible chemicals, could be promising for the treatment of cancer by hyperthermia or other related biomedical applications.

EXPERIMENTAL SECTION

1. Chemicals

Hydrogen tetrachloroaurate(III) trihydrate (HAuCl₄·3H₂O) (from Sigma-Aldrich), Triethylene glycol (TrEG) (ACROS Organics, 98%), 1,3-propanediol (1.3-POD) (ACROS Organics, 98%), Polyvinylpyrrolidone (PVP-K₃₀, Mw= 40000, from Sigma-Aldrich).

2. Methods of characterization

UV-vis absorption measurements were performed with a Perkin-Elmer Lambda 11 UV/VIS spectrophotometer in a wavelength range of 200 - 1000 nm.

For the TEM measurements, the nanoparticles were deposited on carbon coated copper grids by

casting a drop of solution of the nanoparticles. Conventional TEM images were obtained using JEOL JEM-1011 microscope (100kV). HRTEM images were obtained using JEOL JEM 2100 F (200kV) with a spatial resolution of 0.23nm. EDS spectra were recorded in STEM mode. HRTEM images were acquired and processed using the Gatan Digital Micrograph environment.

The images were recorded at the “Centre de Microcaractérisation Raymond Castaing” at the Université Paul Sabatier- Toulouse.

3. Synthetic procedure

Gold nanoparticles (AuNPs) were synthesized by a one-pot polyol process using PVP as the stabilizer. Briefly, 30mL of polyol (TrEG or 1.3-POD) solution, containing 4.9 10⁻⁴mol.L⁻¹ of HAuCl₄·3H₂O and a well defined molar ratio of PVP to the gold precursor (R=nPVP/nAu) were heated to 125°C. The mixture was kept at this temperature for 15 min under continuous mechanical stirring. The nanoparticles were separated from the reaction mixture by repeated centrifugation and ethanol washing steps. Then, the Au NPs were redispersed in ethanol for further analysis. Different attempts have been made to develop simple synthesis of size- and shape-selective anisotropic Au NPs. The different reaction conditions and the predominant anisotropic shapes obtained for each experiment performed are reported in Table I.

RESULTS AND DISCUSSION

Triethylene glycol (TrEG) and 1,3-propanediol (1.3-POD) act as solvents for the gold salt, reducing agent and growth media. According to the

Table I. Synthesis conditions of AuNPs in polyol solvent (TrEG, 1.3-POD) at 125°C, predominant shape and average size of AuNPs obtained.

Samples	Solvent	Molar ratio (R)*	Nanoparticles size (nm)	Predominant shape
A	TrEG	0.03	54 ± 8.5	Hexagonal plate
B	TrEG	0.5	50 ± 7.5	Hexagonal plate
C	TrEG	0.7	110 ± 16.5	Triangular plate
D	TrEG	0.8	55 ± 8.5	Irregular
E	1.3-POD	0.03	27 ± 13	cube
F	1.3-POD	0.7	21 ± 9	cube

R=nPVP/nAu.

literature, the reduction of gold precursor is a multistep process from Au(III) to Au(I) and then to Au(0)[32]. The reduction to Au(I) was evidenced by the fading of the initial yellow solution, which was observed in our experiments at 120°C and 105°C in the case of TrEG and 1.3 POD respectively. Thereafter, the reduction of Au(I) to Au(0) begins, which consequently causes a nucleation followed by a growth process in the solution. These processes were evidenced by the re-coloring of the solutions in blue-brown in the case of TrEG, and purple in 1.3 POD.

PVP acts as stabilizing agent and it is now widely admitted that it is involved in the growth and shaping process by its selective interaction with the different facets of gold crystals, i.e. interaction is preferential with {100} facets reducing thus their free energy [33]. However, Gold triangular nanoprisms with an average edge length of 150 nm were grown in TrEG and small quantities of PVP (PVP/HAuCl₄ molar ratio R=0.05) at 150°C [31], thus questioning the role of the polyol itself. In order to better understand the evolution of our system and the role played by different synthesis factors we attempted several variations of the previous standard experiment.

1. Effect of R= PVP/ HAuCl₄ molar ratio in TrEG as solvent

The set of Au NPs optical absorption properties, obtained by using TrEG as solvent with different molar ratios R, are presented in the UV-vis NIR spectra recorded from the ethanol colloidal solutions (Figure 1). All spectra show two distinct bands: one at ca. 550 nm and a second beyond 700 nm which could be assigned as transverse SPR and longitudinal SPR, respectively. This might indicate the presence of anisotropic nanoparticles in the samples. The colloids synthesized with a molar ratio R = 0.03 (Figure 1 A) display a strong peak at 573nm and a weaker one at 710nm. TEM micrograph of this sample showed the presence of nanoparticles with different shapes and with sizes around 54 ± 8.5 nm (Figure 2 a,b,c). A closer inspection of the TEM image allowed estimating the proportion of different gold shapes on the grid, i.e. 40% of Au hexagonal plates, 35% of Au triangular plates and 25% of AuNPs with other shapes (spherical, icosahedron, dodecahedron...), (Figure 3 A). The smaller size of the nanoparticles obtained in this experiment compared with the standard one [31] could be assigned to the lower

temperature of the reaction, 125°C instead of 150°C, which probably didn't allow the completion of the growth step in this case. The lower temperature was chosen to ensure a slow nucleation step which is known to promote anisotropic shapes [33,34]. The reduced concentration of Au precursor in the synthesis may favor the formation of Au nanoplates also. However, at this early stage of growth the amount of PVP seems to not be high enough to assure the anisotropic growth of all the nanoparticles.

An increase of the molar ratio PVP/Au to R = 0.5 (sample B) is accompanied by a change mainly in the proportion of the two SPR bands in the UV-vis spectra (Figure 1B). Indeed, two quite distinct absorption bands can be observed: a first moderately intense band at 553nm and a second one intense and well symmetrical located in the near infrared range at a wavelength of 745nm. The estimation of the proportion of the different Au NPs shapes revealed in this case 80% of hexagonal plates and 20% of triangular plates (Figure 3B), with a mean particle size of 50 ± 7.5 nm as detailed in the next part (Figure 2 f).

In the case of sample C with a molar ratio R = 0.7, a red shift of both SPR bands was observed, to a wavelength of 620nm and 805nm, respectively (Figure 1C). TEM images revealed AuNPs with a size of 110 ± 16.5 nm (Figure 2 g, h). This size increase could explain the evolution of UV-vis spectra towards the longer wavelengths. Interestingly, the estimated proportions of the

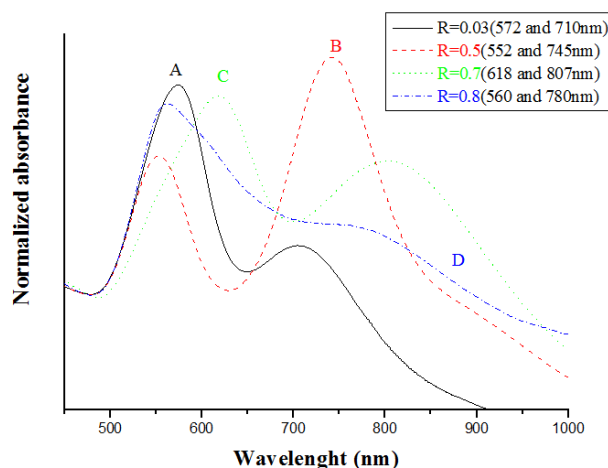


Figure 1. UV/Vis absorption spectra of solutions of Au NPs in ethanol.

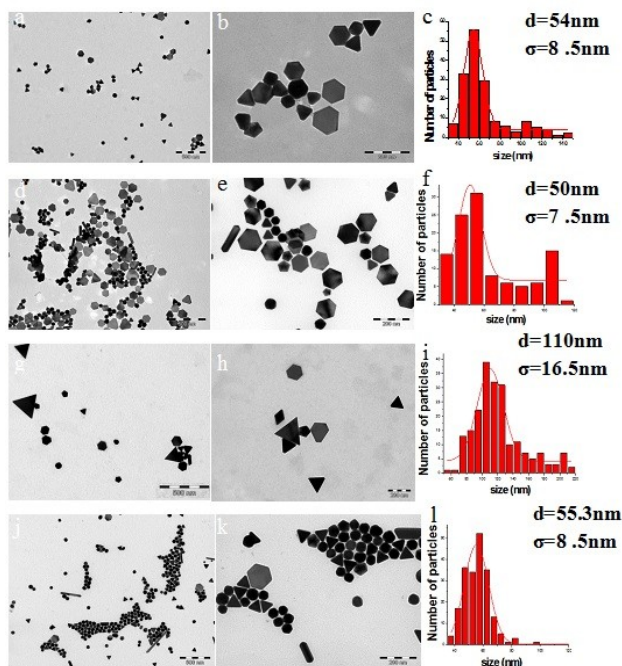


Figure 2. TEM images of Au NPs formed with different PVP/Au molar ratio a,b ($R=0.03$), d,e ($R=0.5$) g,h ($R=0.7$), j,k ($R=0.8$) and their size distribution (respectively c,f, i, l).

different shapes are almost reversed now compared with those found for sample B: the Au triangular plates represent about 70% while the hexagonal plates don't exceed 30% (Figure 2 c). It is noteworthy that a small change in the amount of PVP resulted in a notable change in nanoparticles morphology and size, as shown in Figure 2 g,h. For the sample D ($R = 0.8$) the collapse of the second SPR absorption band (Figure 1D) was observed in agreement with the presence again of a big proportion of icosahedrons and dodecahedrons estimated to 72% with a mean size of 55.3 ± 8.5 nm. In this sample the proportion of hexagonal plates no longer exceeds 7%, while the other Au NPs were triangular plates (Figure 3D and Figure 2 j, k, l). In this case the quantity of PVP should be high enough to allow its adsorption on the whole surface of growing nanoparticles. Therefore the anisotropic growth is retarded. Figure 3 reports the estimated proportions of different Au NPs shapes observed for each sample. It is obvious that with a single synthetic approach it is possible to shift the positions of the SPR peaks of gold nanoparticles through the near infrared region. This shift could be dominated by the variation of the amount of different shapes in the sample.

2. Characterization of sample B

Sample B was then selected as the most adapted one for the envisaged application due to the strong SPR absorption band exhibited in the infrared region. TEM images of the particles (Figure 4a) indicated that there are mainly hexagonal nanoplates. The size distribution indicated an average size of about 50 ± 7.5 nm (Figure 4b). The Energy-dispersive X-ray spectroscopy (EDX) confirmed that the nanoparticles consist of only gold. (Figure 4c).

HRTEM images performed on a gold nanoplate of hexagonal shape (Figure 4 d and f) showed lattice planes proving the crystallinity of the sample. The FFT shown in Figure 4e exhibits 6 folds symmetry, corresponding to the $\{220\}$ reflections of fcc gold crystal oriented in the $[111]$ direction.

The images taken from the side face of gold nanoplate showed that the crystalline structure admits internal defects (Figure 4 f,g). The FFT exhibited splitted reflections and probably appearance of forbidden reflections which can be related to the presence of stacking faults which would also direct the growth of the particles.

Among the most requested Au NPs characteristics for their use in biomedical application as hyperthermia mediators is their stability against aggregation. To emphasize such stability of the nanoparticles, an optical study was performed. The UV-vis spectrum of sample B conserved as a colloidal solution in the fridge during six months indicated no spectral broadening of the plasmon bands thus confirming the stability of these Au NPs (Figure 4l).

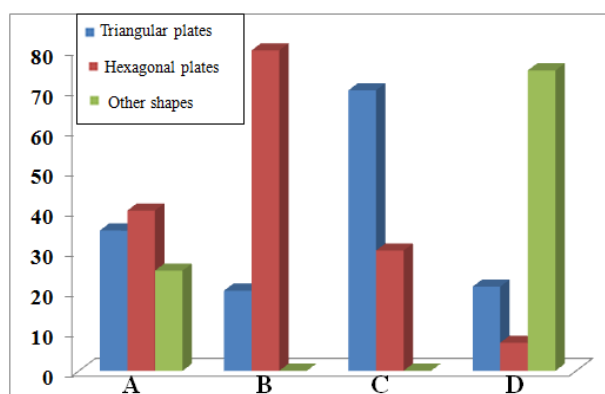


Figure 3. Morphological fraction of NPs at different PVP/Au molar ratio: A ($R = 0.03$), B ($R = 0.5$), C ($R = 0.7$) and D ($R = 0.8$) samples.

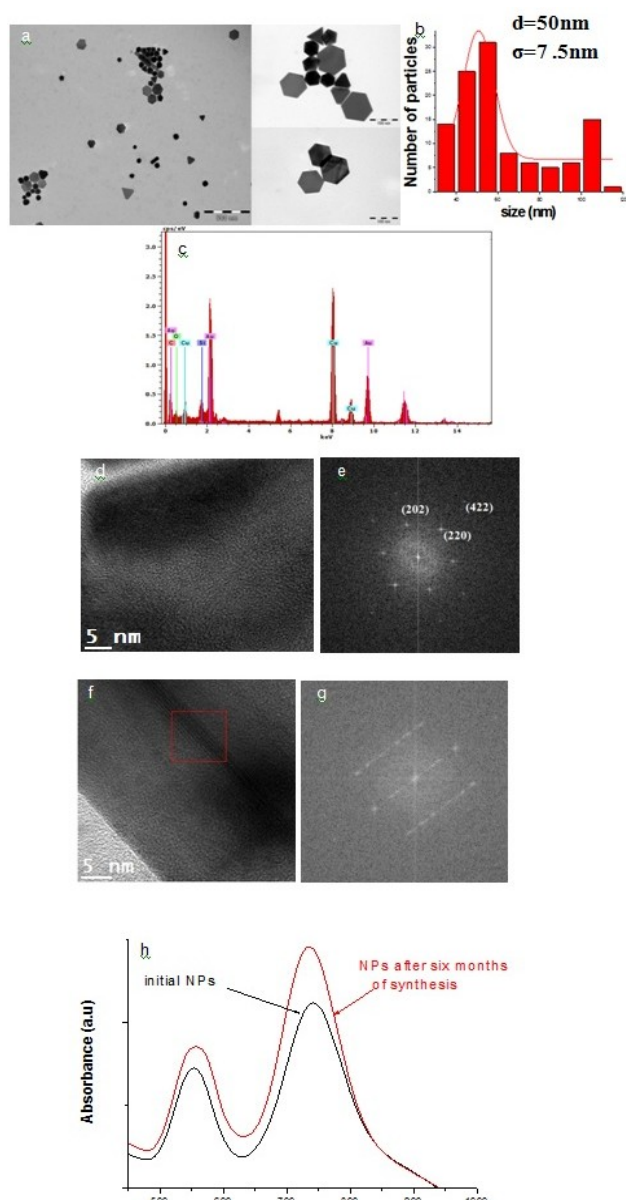


Figure 4. TEM image of the synthesized NPs in TrEG (a) scale: 500nm, size distribution (b), Energy dispersive spectrum (c), HRTEM images taken from the front face (d) scale: 5 nm and the side face (f), scale: 5 nm of a selected nanoparticle with the corresponding FFT patterns (e) and (g), and comparative UV-vis spectra of colloidal solutions directly after synthesis and after six months (h).

3. Effect of the the polyol solvent

We have shown above that during a polyol synthesis, the growth of the particles could be oriented towards a privileged shape and size by modifying the PVP/Au molar ratio. We then studied the influence of the solvent by performing new experiments using 1,3-POD instead of TrEG.

The effect of the solvent was followed by comparing the optical response of the colloidal solution obtained. For this comparative study, we focused on the synthesis of samples A and C ($R = 0.03$ and 0.7 for samples A and C, respectively) and we investigated if the change in solvent caused changing in the AuNPs shape and size.

In comparison with the samples A and C synthesized in TrEG, the UV-vis spectrum of both samples synthesized in 1,3-POD (Samples E and F, respectively) showed a unique symmetric absorption peak at 552 nm and 546 nm, respectively (Figure 5). The disappearance of the longitudinal SPR peak observed could result from a change in the morphology of the nanoparticles synthesized in 1,3-POD.

The TEM images of sample E showed truncated cubic nanoparticles at an estimated percentage of 40%, with triangular plates and quasi-spherical nanoparticles at a percentage of about 30% for these two types of shape. Note that we did not observe Au hexagonal plates (Figure 6 a,b). It is noteworthy that a small size of 27 ± 13 nm was obtained for the Au nanocubes. Such a size range is scarcely reported for cubic Au nanoparticles prepared by a polyol process.

In the case of sample F, the TEM images (Figure 7 a,b) revealed that the sample mainly contain cubic particles with once again a remarkable small size of 21 ± 9 nm (Figure 7 c). These observations are consistent with the UV-vis data recorded and are in agreement with those calculated for the cubes of

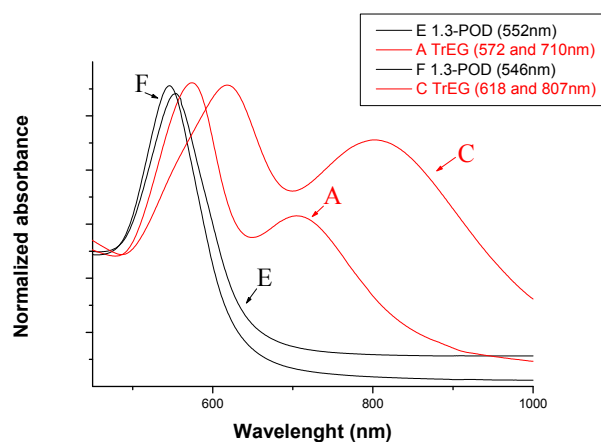


Figure 5. Comparative UV-vis spectra between NPs synthesized in TrEG and 1,3-POD with the same PVP/Au molar ratio (respectively samples A, E and C, F).

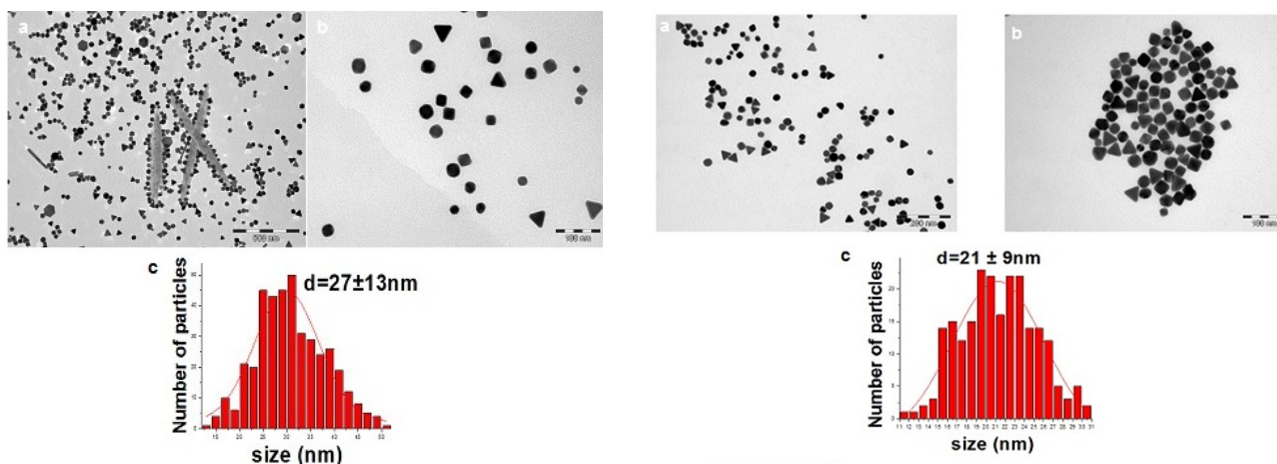


Figure 6. TEM images of AuNPs - Sample E (a: scale 500nm, b: scale 50 nm), size distribution (c).

similar sizes [35]. Once again, the EDX confirmed that the nanoparticles consist of only gold (Figure 7 d).

FFT analysis of an HRTEM image of a Au nanocube showed only the (111) and the corresponding (222) lattice planes spacing of the fcc gold crystal oriented in the [011] direction.

The experiments performed in 1.3 POD clearly indicated the nanoparticles shape dependence on the reaction solvent. Indeed, the reduction of HAuCl_4 in TrEG was slower than in 1.3 POD (temperature of reduction was of 120°C in TrEG versus 105°C in 1.3 POD). Moreover the temperature of reaction was intentionally decreased in order to advantage kinetic condition of growth. Kinetic control has been demonstrated as a simple and versatile approach to the shape-controlled synthesis of metal nanostructures. When the reduction becomes slow enough, kinetic control will take over in both nucleation and growth: seeds with stacking faults can nucleate and then growth into nanoplates. In TrEG, the presence of staking faults was evidenced on the final plates. This supports the hypothesis of nucleation and formation of seeds in the kinetic regime. These initial seeds which also probably contain stacking faults that will further evolve into Au nanoplates. During growth, the plates may either keep the triangular shape or be truncated, which depends on the ratio of {111} to {100} facets on the side face [36]. In contrast, faster reduction rates are necessary for the formation of single crystal seeds

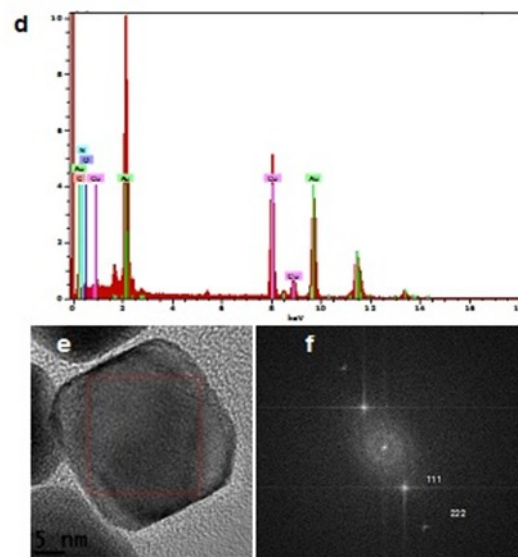


Figure 7. TEM images of the synthesized NPs (a scale: 200nm; b scale: 100nm), size distribution (c), Energy dispersive spectrum (d), HRTM image of truncated nanocubes (e scale :5nm), FFT pattern (f).

and further thermodynamically stable shapes as it might be the case when the reduction was performed in 1.3 POD.

Even, the morphology of a crystal is determined by the interplay of many parameters, here the shape of the final Au NPs seems to be determined by the initial nucleation step and thus the morphology of the initial seeds [37]. As far as PVP is concerned, it seems to be more involved in the growth process ones the initial seeds were already formed, due to its stronger affinity for the {100} facets than for the {111} ones. However, it was postulated that in the case of Au this selective affinity is less pronounced than in the case of Ag [33], which could explain the formation, in most of the cases,

of more than only one shape in the samples. As a result, attempt to tighten the shape distribution in the case of Au involved for example the addition of Ag^+ and Br^- ions in the reaction medium [38,17,32]. It is however clear that any successful synthesis needs a careful control over the nucleation and growth steps.

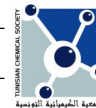
CONCLUSION

A low temperature polyol method was reported here with either TrEG or 1.3 POD as a solvent and reducing agent. The effect of the solvent was revealed as dominant in the shape orientation of the final nanoparticles by tuning the reduction rate of the gold salt. Thus the shape of the gold nanoparticles seems to be promoted by the nucleation step. In TrEG, triangular or hexagonal nanoplates were the predominant shapes while in 1.3 POD the cubic shape appeared as favored. Additional studies suggested that the PVP is not greatly involved in the shape exhibited by the final nanoparticles, but it helps to stabilize and to conduct the growth of the initial seeds towards the final shape. Finally, it should be mentioned the remarkable size range obtained for the Au nanoparticles here described. A future plan could be the functionalization of their surface in order to evaluate them in biomedical applications.

Acknowledgements: The authors would like to thank the financial support of Campus France under project PHC-Utique 32789YK. University of Carthage, University Paul Sabatier-Toulouse and CNRS are also acknowledged for financial support.

REFERENCES

- [1] Liu, F. K.; Chang, Y. C.; Koa, F. H.; Chub, T. *C.Mater. Lett.* **2004**, *58*, 373-377.
- [2] Hassenkam, T.; Moth-Poulsen, K.; Stuhr-Hansen, N.; Norgaard, K.; Kabir, M. S.; Bjornholm, T. *Nano Lett.* **2004**, *4*, 19-22.
- [3] Prasad, P. N. *Wiley-Interscience: Hoboken, NJ*, **2012**.
- [4] Perrault, S. D.; Chan, W. C. W. *J. Am. Chem. Soc.* **2009**, *131* (47) 17042-17043.
- [5] Chen, G. Y.; Qiu, H. L.; Prasad, P. N.; Chen, X. Y. *Chem. Rev.* **2014**, *114* (10) 5161-5214.
- [6] Huang, C.-C.; Chang, P.-Y.; Liu, C.-L.; Xu, J.-P.; Wu, S.-P.; Kuo, W.-C. *Nanoscale.* **2015**, *7*, 12689-12697.
- [7] Burda, C.; Chen, X. B.; Narayanan, R.; El-Sayed, M. A. *Chem. Rev.* **2005**, *105*, 1025-1102.
- [8] Kelly, K. L.; Coronado, E.; Zhao, L. L.; Schatz, G. C. *J. Phys. Chem. B.* **2003**, *107*, 668-677.
- [9] Chil Seong Ah, Yong Ju Yun, HyungJu Park, Wan-Joong Kim, Dong Han Ha, and Wan Soo Yun. *Chem. Mater.* **2005**, *17*, 5558-5561.
- [10] Jang, B.; Kim, Y. S.; Choi, Y. *Small.* **2011**, *7*, 265-270.
- [11] Sotiriou, G. A.; Starsich, F.; Dasargyri, A.; Wurnig, M. C.; Krumeich, F.; Boss, A.; Leroux, J.; Pratsinis, S. E. *Adv. Funct. Mater.* **2014**, *24*, 2818-2827.
- [12] Chih-Chia Huang, and Tzu-Ming Liu. *ACS Appl. Mater. Interfaces.* **2015**, *7*, 25259-25269.
- [13] Ungureanu, C.; Kroes, R.; Petersen, W.; Groothuis, T. A. M.; Ungureanu, F.; Janssen, H.; van Leeuwen, F. W. B.; Kooyman, R. P. H.; Manohar, S.; Van Leeuwen, T. G. *Nano Lett.* **2011**, *11*, 1887-1894.
- [14] Yanlei Liu, Meng Yang, Jingpu Zhang, Xiao Zhi, Chao Li, Chunlei Zhang, FeiPan, Kan Wang, Yuming Yang, Jesus Martinez de la Fuente and Daxiang Cui. *ACS Nano.* **2016**, *10*, 2375-2385.
- [15] Shankar, S. S.; Rai, A.; Ankamwar, B.; Singh, A.; Ahmad, A. *Nat. Mater.* **2004**, *3*, 482.
- [16] T. K. Sau and C. J. Murphy. *Langmuir.* **2004**, *20*, 6414-6420.
- [17] F. Kim, S. Connor, H. Song, T. Kuykendall, and P. D. Yang. *Angew. Chem. Int. Ed.* **2004**, *43*, 3673-3677.
- [18] S. S. Shankar, A. Rai, B. Ankamwar, A. Singh, A. Ahmad, and M. *Nat. Mater.* **2004**, *3*, 482-488.
- [19] J. Zhang, H. Liu, Z. Wang, and N. Ming. *Adv. Funct. Mater.* **2007**, *17*, 3295-3303.
- [20] Babak Nikoobakht and Mostafa A. *Chem. Mater.* **2003**, *15*, 1957-1962.
- [21] Catherine J. Murphy, Anand M. Gole, John W. Stone, Patrick N. Sisco, Alaadin M. Alkilany, Edie C. Goldsmith, Sarah C. Baxter. *Accounts of Chemical Reserch.* **2008**, *41*, 1721-1730.
- [22] Tsunoyama, H.; Ichikuni, N.; Sakurai, H.; Tsukuda, T. *J. Am. Chem. Soc.* **2009**, *131*, 7086-7093.
- [23] Peng, C.; Lo, S. H. Y.; Wan, C. C.; Wang, Y. Y. *Colloids Surf.* **2007**, *308*, 93-99.
- [24] Lan, J. L.; Wan, C. C.; Wang, Y. Y. *J. Electrochem. Soc.* **2008**, *155*, 77-83.
- [25] Kumar, P. S.; Pastoriza-Santos, I.; Rodríguez-González, B.; Abajo, F. J. G. d.; Liz-Marzañ, L. M.; Javier García de Abajo, F. *Nanotechnology* **2008**, *19*, 015-606.
- [26] Daeha Seo, Ji Chan Park, and Hyunjoon Song. *J. Am. Chem. Soc.* **2006**, *128*, 14863-14870.
- [27] Meherzad F. Variava, Tamara L. Church, Andrew T. Harris and Andrew I. Minett. *J. Mater. Chem. A.* **2013**, *1*, 8509.
- [28] Yugang Sun and Younan Xia. *SCIENCE.* **2002**, *298*.
- [29] Marek Grzelczak, Jorge Pe' rez-Juste, Paul Mulvaney and Luis M. Liz-Marza' n. *Chem. Soc. Rev.* **2008**, *37*, 1783-1791.



- [30] Cristina E. Hoppe, Massimo Lazzari, IvánPardiñas-Blanco and M. Arturo López-Quintela. *Langmuir*. **2006**, 22(16), 7027-7034
- [31] Amine Mezni, Thameur Dammak, Anis Fkiri, Adnen Mlayah, Younes Abid, and Leila Samia Smiri. *J. Phys. Chem. C*. **2014**, 118 (31), 17956-17967.
- [32] Walter F. Paxton, Paul T. Baker, Timothy R. Kline, Yang Wang, Thomas E. Mallouk, and Ayusman Sen. *J. Am. Chem. Soc.* **2006**, 128, 14881-14888.
- [33] Younan Xia, Yujie Xiong, Byungkwon Lim, Sara E. Skrabalak. *Angew. Chem. Int. Ed.* **2009**, 48, 60-103.
- [34] Yujie Xiong, Isao Washio, Jingyi Chen, Honggang Cai, Zhi-YuanLi, and YounanXia. *Langmuir*. **2006**, 22 (20), 8563-8570.
- [35] Daeha Seo, Choong Il Yoo, Ji Chan Park, Seung Min Park, Seol Ryu, and Hyunjoon Song. *Angew. Chem. Int. Ed.* **2008**, 47, 763 -767.
- [36] Yujie Xiong, Joseph M. McLellan, Jingyi Chen, Yadong Yin, Zhi-Yuan Li, and Younan Xia. *J. Am. Chem. Soc.* **2005**, 127 (48), 17118-17127.
- [37] Yujie Xiong, Isao Washio, Jingyi Chen, Martin Sadilek, and Younan Xia. *Angew. Chem. Int. Ed.* **2007**, 46, 4917 -4921.
- [38] Franklin Kim, Stephen Connor, Hyunjoon Song, Tevye Kuykendall, and Peidong Yang. *Angew. Chem.* **2004**, 116, 3759 -3763.